

# The WinGeol Lamination Tool: new software for rapid, semi-automated analysis of laminated climate archives

Michael C. Meyer,<sup>1\*</sup> Robert Faber<sup>2</sup> and Christoph Spötl<sup>1</sup>

(<sup>1</sup>Leopold-Franzens-Universität Innsbruck; Institut für Geologie und Paläontologie, Innrain 52, 6020 Innsbruck, Austria; <sup>2</sup>TerraMath, Heiligenstädterstraße 107, 1190 Vienna, Austria)

Received 2 July 2005; revised manuscript accepted 4 January 2006



**Abstract:** Geological and biological archives showing an annually laminated internal structure are currently top priority in palaeoclimate research, as they are recognized as very high-resolution archives of environmental change. Also, the annual origin of laminations can be validated by absolute age dating or by using instrumental data for the most recent period. Microscopic laminae may span several hundreds to thousands of years and frequently reveal a high degree of internal growth variability. Quantitative examination of laminations using transmitted-light or epifluorescence microscopy is thus a tedious task and may be partly automated. We developed a software (WinGeol Lamination Tool) using C++ capable of semi-automatically detecting and measuring individual lamina thicknesses in archives showing large internal growth variability. The Lamination Tool enables the operator to efficiently and quantitatively examine laminae down to the micron scale and it was successfully tested on a variety of annually banded samples.

**Key words:** Digital image analysis, algorithm, RGB curve, software, annual lamination, thin section, WinGeol Lamination Tool.

## Introduction

Lamination is a widespread growth phenomenon in many geological and biological materials. Examples of macroscopic lamination include tree rings, varved lake sediments, bivalves, ice cores and reef corals. The origin and growth mechanism of lamination, although complex in detail and different for each environment, is generally driven by processes on subannual to multiannual timescales.

Laminations of annual origin (annually laminated or annually banded archives) are recognized as very high-resolution archives of environmental change and their annual origin can be validated using instrumental data for the most recent period of the last 200 years (eg, Hughen *et al.*, 2000, Frisia *et al.*, 2003). In certain areas, laminated sedimentary sequences provide continuous millennial-scale records, eg, the marine lateglacial sediments in the Cariaco basin (Hughen *et al.*, 2004), Holocene speleothems from Oman (Fleitmann *et al.*, 2004), or varved lake sediments from Germany (Hajdas *et al.*, 1995; Zolitschka, 1998) or Finland (Ojala and Alenius, 2005).

In many cases examination of annually laminated successions requires microscopic techniques and the process of

lamina counting and thickness measurement remains a tedious task. To aid or automate lamina analysis several numerical techniques have been developed, all based upon digital image processing. A variety of software is in use for counting tree rings (eg, Varem-Sanders and Campbell, 1996; Conner *et al.*, 2000; RinnTech, 2002) but it is not sufficiently versatile for convenient use on sediment cores or petrographic thin sections. Algorithms for automated lamina recognition on surfaces of sediment cores (Schaaf and Thurow, 1994) and petrographic thin sections (Zolitschka, 1996) work reliably for only regularly layered sediments. The lamina counting tool presented by Francus *et al.* (2002) assists manual counting but is impracticable for more complex or curved laminae. Seelos and Sirocko (2005) recently suggested a particle-size measurement technique to analyse thin sections of clastic sediments, optimized for laminated sediments of maar lakes.

As the existing numerical techniques hold inherent limitations, the process of lamina counting and measurement still remains a very tedious task, especially in the case of slow-growing speleothems where micron-scaled annual growth layers are frequent, as shown by UV illumination. We thus developed a software tool to efficiently and accurately analyse long and complex laminated sequences but we ensured that a

\*Author for correspondence (e-mail: michael.meyer@uibk.ac.at)

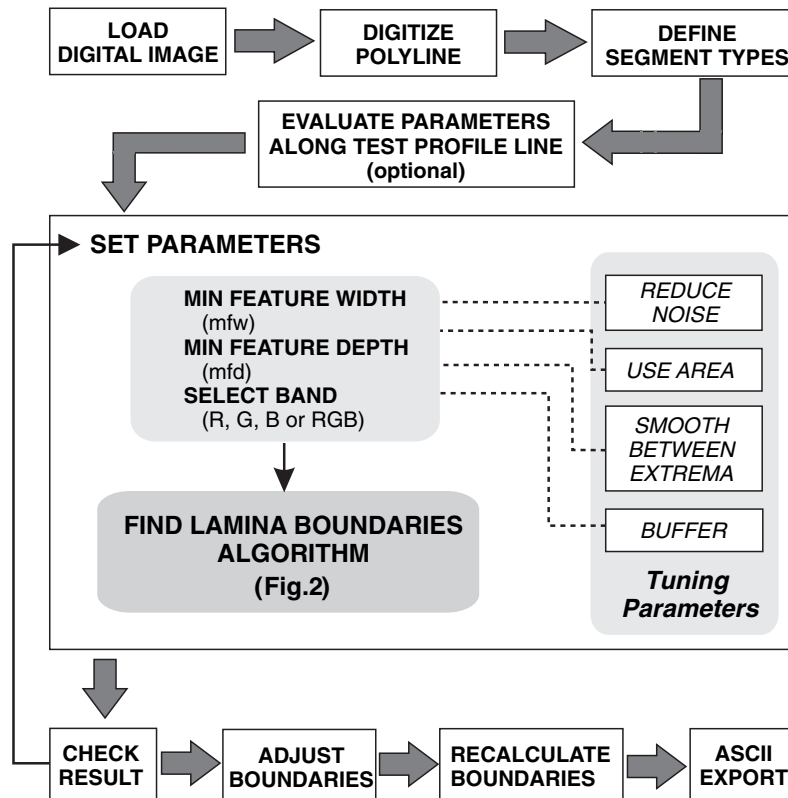


**Figure 1** Workflow of the WinGeol Lamination Tool. The detection parameters ‘minimum feature width’, ‘minimum feature depth’ and the selection of a colour band are mandatory, whereas the tuning parameters are optional

high degree of control remains with the operator to handle even high internal growth variability.

Our algorithm has also been successfully applied to other laminated archives and achieves good results in well- to moderately well-resolved laminated sequences.

## The software

The WinGeol Lamination Tool, written in C++, is capable of semi-automatically detecting and measuring laminae based on RGB or greyscale curves obtained from digital images of thin sections or sediment surfaces. WinGeol is a software package designed for a wide range of geoscientific applications and the Lamination Tool is programmed as an add-on to this main software package.

The Lamination Tool uses graphic libraries to dynamically readout and memorize data produced during the progressive calculation/detection process. General data handling is assured by GRbase libraries (vector and grid operations, ©TerraMath) whereas lamina operations are executed by specifically developed algorithm and Lamination Tool libraries (©TerraMath). Separate layers are used for grid data (digital images), vector data (manually digitized polylines) and text (annotations) and a layer tree window allows to easy management of these different data layers.

## Acquiring digital images

Digital images from petrographic thin sections, drill cores, sediment surfaces or sediment slabs are obtained by means of a digital camera mounted on a microscope or via a flat-bed scanner. For lamina analysis high quality images are required, ensuring that each lamina is represented by at least several

pixels. For microscopic lamination we use an X–Y microscope stage to precisely align transects across individual thin sections. Images are imported and stitched together using the software tool; alternatively, stitching can be done using conventional software packages for image processing (eg, Adobe Photoshop). Our software is optimized to rapidly process raster data up to one gigabyte, thus enabling the operator to efficiently handle long laminated sequences. For each image colour inversion, channel combinations and histogram modifications can be performed as necessary and saved for the subsequent lamina detection process.

## Preparatory steps

The workflow of the lamination analysis and the underlying principles of the find-boundary algorithm (fb-algorithm) are illustrated in Figures 1 and 2. The workflow involves first loading a digital image (grid layer) into the two-dimensional (2D) workspace and generating a vector layer upon which digitizing is permitted. The digital image can be sized to user-specified units (eg, micronmeter, millimeter, etc.) by applying the correct cell size. Second, the user digitizes a polyline by defining data-, no-data- and link-segments in order to maintain control over laminated and non-laminated sequences. Data segments that cover the laminated sequences of the sample are digitized perpendicularly to the lamina boundaries. Link segments connect two data segments with each other and no-data segments are used where lamination is obscured or absent. The RGB curve is obtained from the digital image along the course of the polyline and can be visualized in the profile-view window. Usually the x-axis of this profile window carries user-specified units whereas the y-axis comprises the greyscale or colour intensity (pixel values 0 to 255). In the case of RGB images each colour band is displayed as an individual

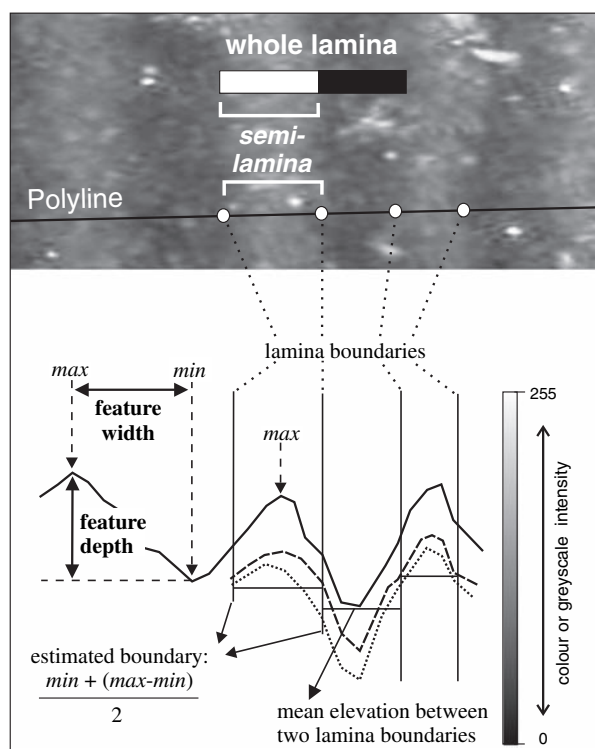


**Figure 2** Principle of the find-boundary algorithm. The algorithm compares neighbouring pixel values relatively with each other and calculates minima and maxima along the RGB curve. Line formatting indicates colour band: continuous, green; dashed, red; dotted, blue. During an iterative process the RGB curve is screened for features of a certain minimum width and minimum depth and the algorithm places laminae boundaries half way between the minimum and the maximum. Real (whole) laminae are obtained by summing up one dark and one light semi-laminae during the ASCII export (for details see text)

intensity curve in the profile-view window and all three bands are referred to as the RGB curve (eg, Figure 3b and c). By zooming and moving along the polyline in the 2D workspace the details of the RGB curve are shown simultaneously in the profile-view window. The fb-algorithm runs along the data-segments only and uses the RGB curve as computational base to suggest lamina boundaries to the operator.

## The fb-algorithm

In the first step the fb-algorithm compares the RGB values of neighbouring pixel and calculates minima and maxima along the RGB curve. Troughs and peaks are caused by variation in greyscale or colour intensity in the RGB curve and are referred to as RGB features. The horizontal and vertical distances between successive minima and maxima are memorized as feature widths and feature depths, respectively (Figure 2). In the next step the RGB curve is screened for features of a certain minimum width and minimum depth. The minimum feature width (mfw) and the minimum feature depth (mfd) are input parameters that have to be specified by the operator. Features greater than these minimum values are recognized as valid and a lamina boundary is placed half way between the minimum and the maximum (Figure 2). Essentially, the fb-algorithm places boundaries at light–dark and dark–light transitions and thus detects semi-laminae from which real lamina thicknesses (whole lamina) are obtained during the final ASCII export.

Our algorithm ‘morphologically’ screens the RGB curve for features of a certain size by comparing neighbouring pixel values relatively with each other and works with ‘sizes of RGB features’ rather than the conventional approach of calculating a curve function. The lamina detection process is thus straightforward and robust.

## Setting parameters

The optimal input parameters for running the fb-algorithm (mfw and mfd) can be directly measured from the RGB curve in the profile-view window using the cursor. Alternatively, these values can be determined via an evaluation process whereby the steps of the fb-algorithm are inversely applied: the operator digitizes a short polyline placing a node on each lamina boundary and the *Evaluate Function* (Figure 1) calculates the minimum and average feature width and depth from the RGB curve for which the lamina boundaries were defined.

Several further parameters have been implemented for tuning the fb-algorithm (Figure 1) in order to enhance the robustness of the detection routine and to process different types of lamination accurately.

The *Reduce Noise* function is a median filter applied to the RGB curve prior to the fb-algorithm calculation. The function has a smoothing effect on the RGB curve and is useful for example where inclusions interfere with laminae and disturb the RGB signal.

The *Use Area* function calculates the surface area for each RGB feature to determine lamina boundaries rather than filtering by fixed mfw and mfd values. This function improves the results, for example where thin and dark semi-laminae alternate with broad and bright semi-laminae. The RGB signal of the thin and dark semi-laminae has narrow RGB features of high amplitude. These are frequently overlooked using fixed mfw and mfd values, because the mfw is too low to accept as valid RGB features although the amplitude is remarkably high. The *Use Area* function compares the surface area of RGB features as derived from their line-integrals. RGB features with surface areas equal to or greater than that of the normal curve (defined by the mfw and the mfd) are accepted as valid semi-laminae and thus detected independently from the mfw value.

The *Smoothing* function is a median filter applied during the fb-calculation before the lamina boundaries are placed between a minimum and a maximum value. A more sinusoidal curve results from this calculation step, after which the lamina boundaries are placed upon the smoothed RGB curve. Test runs for different lamination types using low to moderately high smoothing factors indicate higher accuracies for the final results. The smoothing factor is specified by the operator. A value of 0 implies no smoothing and a value of 1 (default) causes each pixel along the RGB curve to be averaged with one pixel before and after it prior to placing the lamina boundaries.

The *Buffer* function incorporates the RGB values of pixel perpendicular to the polyline and calculates their average. The operator specifies the buffer value, which is the number of pixel to be included left and right of the polyline; eg, a buffer of 20 broadens the polyline to a strip of 40 pixel for running the fb-algorithm. The buffer function generally improves the robustness of the lamina detection process and high buffer values allow the operator to grasp even faint laminae.

In addition to these tuning parameters the *Colour Band* (red, green, blue or all) can be chosen by the operator if RGB images are used for the lamina analysis. In many samples intensity curves of individual colour bands differ in terms of their

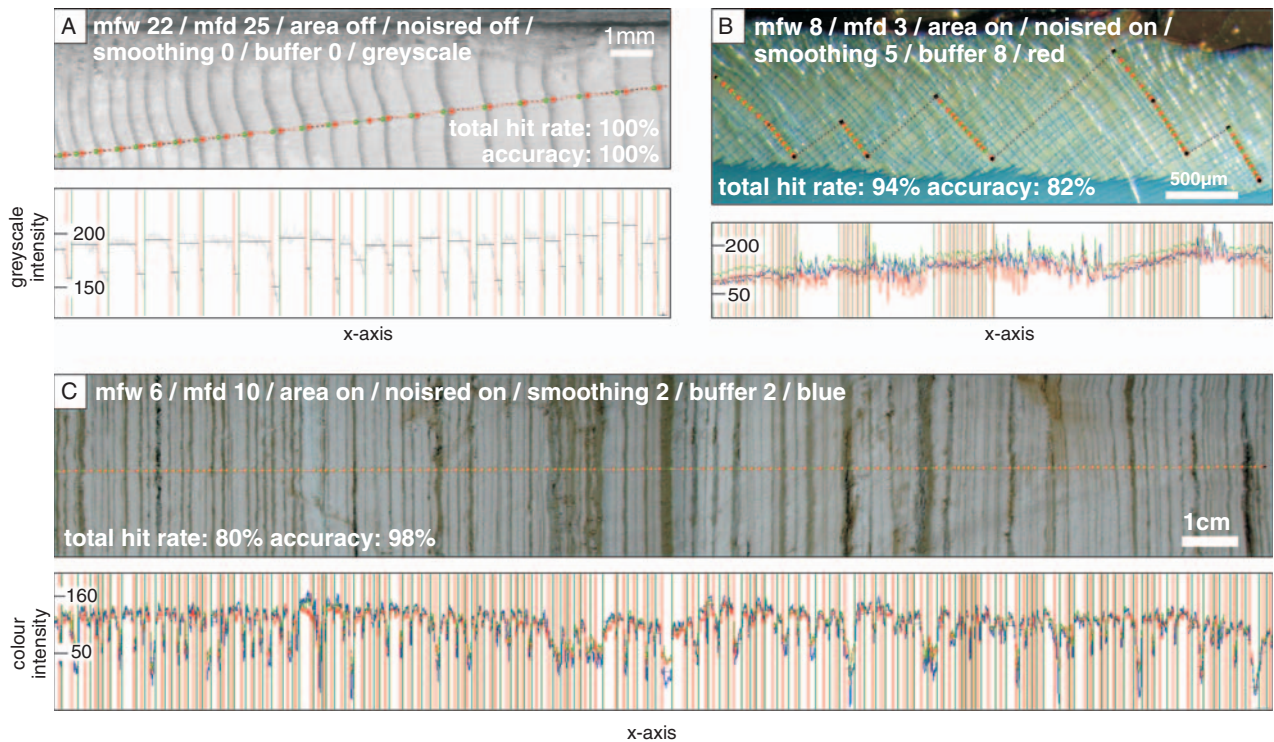


**Figure 3** Performance of the fb-algorithm in different laminated archives. (A) Drill core of a fir, width of annual growth rings: 50–1000  $\mu\text{m}$ . Photo courtesy M. Kaufmann. (B) Lacustrine pearl oyster (*Magnifera magnifera*), thickness of annual growth bands 20–70  $\mu\text{m}$ . Photo courtesy B. Schöne. (C) Banded lake sediments, Lisan Formation, Israel. Images were obtained from the sediment surface of a cleaned outcrop. Photo courtesy N. Waldmann

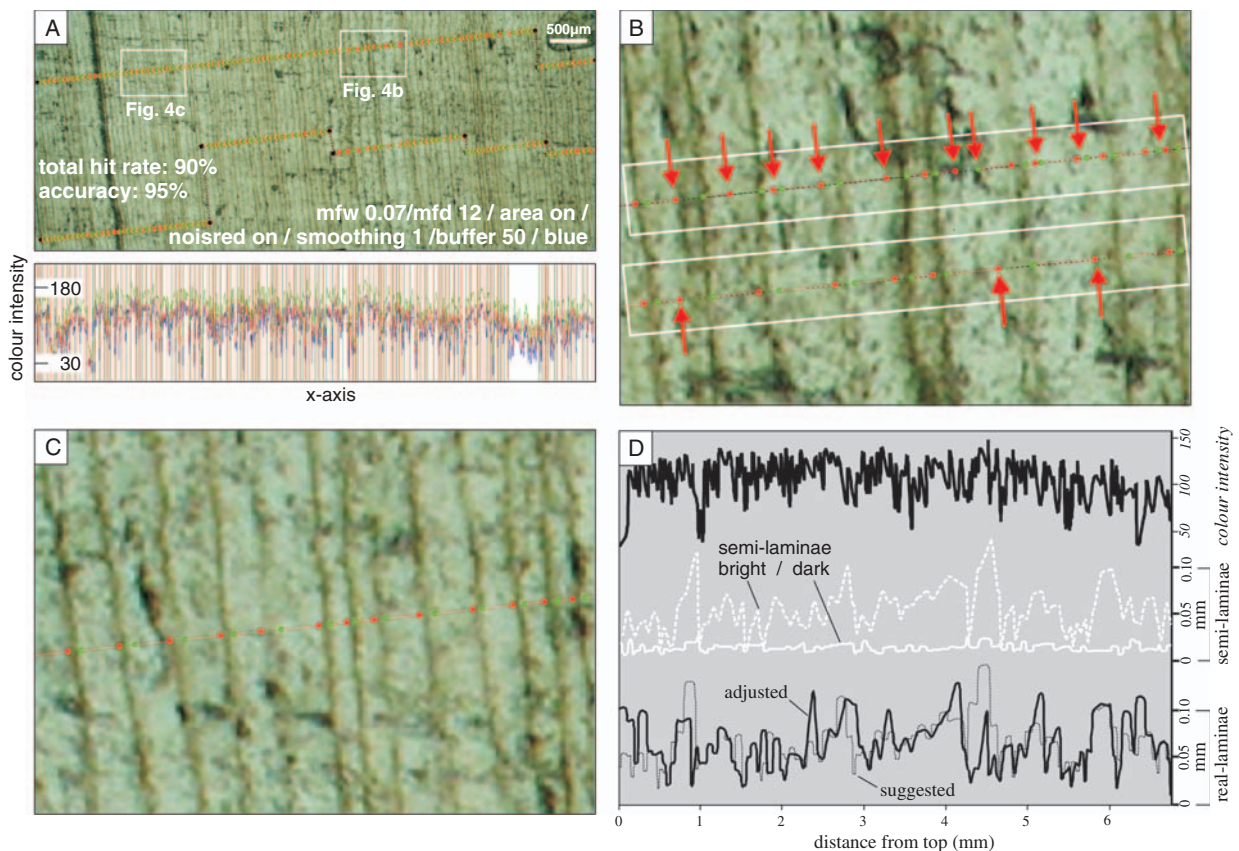


**Figure 4** Performance of the fb-algorithm in laminated speleothems. Annually laminated stalagmite from Savi Cave (Italy). (A) Photomicrograph covers *c.* 110 annual laminae. RGB curves were obtained along user-defined polylines. (B) The polylines are buffered using a value of 50 (white rectangles). Along the upper polyline inclusions cause several surplus boundaries (arrows). Moving the profile away from inclusion-rich areas (lower polyline) increases the total hit rate significantly. (C) In inclusion-poor areas the tuned fb-algorithm achieves accurate results. (D) Intensity variations of the blue colour band (bold black curve), thickness variation of semi-laminae (white curves) and real (whole) laminae (thin black curve) versus depth. Dotted black curve represents the uncorrected lamina boundaries as suggested by the fb-algorithm. Photos A–C courtesy S. Frisia and A. Borsato

amplitude. Using a colour band, which represents lamination as a high amplitude signal, thus improves the results in some samples.

Optimal results are obtained by an accurate tuning of these detection parameters for each lamination type and by choosing an appropriate colour channel.

## Manual adjustments

The fb-algorithm suggests lamina boundaries as alternating red and green dots in the 2D workspace and these lamina boundaries are displayed as vertical bars in the profile-view window (Figures 3 and 4). The results can be evaluated and each boundary can be adjusted manually by the operator in order to distinguish between annual and subannual layering, to delete surplus boundaries, to add missing boundaries or to shift inaccurately placed lamina boundaries.

The suggested boundaries are stored on a separate vector layer (LAM-layer) on which manual adjustments can be performed. The LAM-layer with the manually corrected lamina boundaries must be recalculated to obtain correct intensity values and lamina thicknesses as the position of the suggested boundaries might have changed.

Finally, the total number and thickness of the laminae and semi-laminae, and the greyscale or RGB variation versus depth can be exported as an ASCII file for subsequent visualization and interpretation using common statistical software packages.

## Examples and case studies

We tested our software on six laminated samples from four different climate archives (Figures 3–5): tree rings of a silver fir (Figure 3A), a lacustrine pearl oyster with annual accretion bands (Figure 3B), banded lake sediments of the Lisan Formation (Figure 3C), a laminated speleothem from Savi Cave (Figure 4), and a complexly laminated stalagmite from Ernesto Cave recorded both in transmitted-light (Figure 5A) and epifluorescence (Figure 5B). We calculated the total hit rate and accuracy for each laminated sample to estimate the performance and quality of the results obtained using the automated detection routine. Following tuning of the detection parameters the total hit rate and the accuracy are derived from the semi-lamina boundaries as suggested by the fb-algorithm. The total hit rate incorporates the correctly placed first-hit boundaries, subtracts the surplus and missed boundaries and expresses the result as a percentage of the real lamina boundaries:

$$\text{Total hit rate} = \frac{\text{first hit} - (\text{too less} + \text{too much})}{\text{real number of semi-laminae}} * 100\% \quad (1)$$

The accuracy refers to the ability of the fb-algorithm to position the suggested lamina boundaries precisely on dark–light transitions and thus to measure semi-laminae thicknesses correctly. We calculated the accuracy for each sample as the precisely positioned lamina boundaries expressed as percentage of the first-hit boundaries.

### Dendrochronology

The annual growth rings of the fir are formed by bright spring wood alternating with dark summer wood (Figure 3A). The greyscale profile is characterized by plateau-like features with values of about 200 intersected by sharp drops down to values of 140 for the dark summer wood horizons. The laminae are

detected accurately by a mfw of 22 and a mfd of 25 (pixel values) and no further tuning of the detection parameters is needed.

### Sclerochronology

The lacustrine pearl oyster clearly shows a zone of annual accretion in the outer shell (Figure 3B). Polysaccharides (dyed blue) are concentrated along the annual growth cessations (B. Schöne, personal communication, 2005). Lamination in the profile view is characterized by high amplitude variations best seen in the red colour channel. The polyline consists of five data segments connected by link segments. The total hit rate is good (94%) and the accuracy of 82% implies that two out of ten semi-lamina boundaries need adjustment.

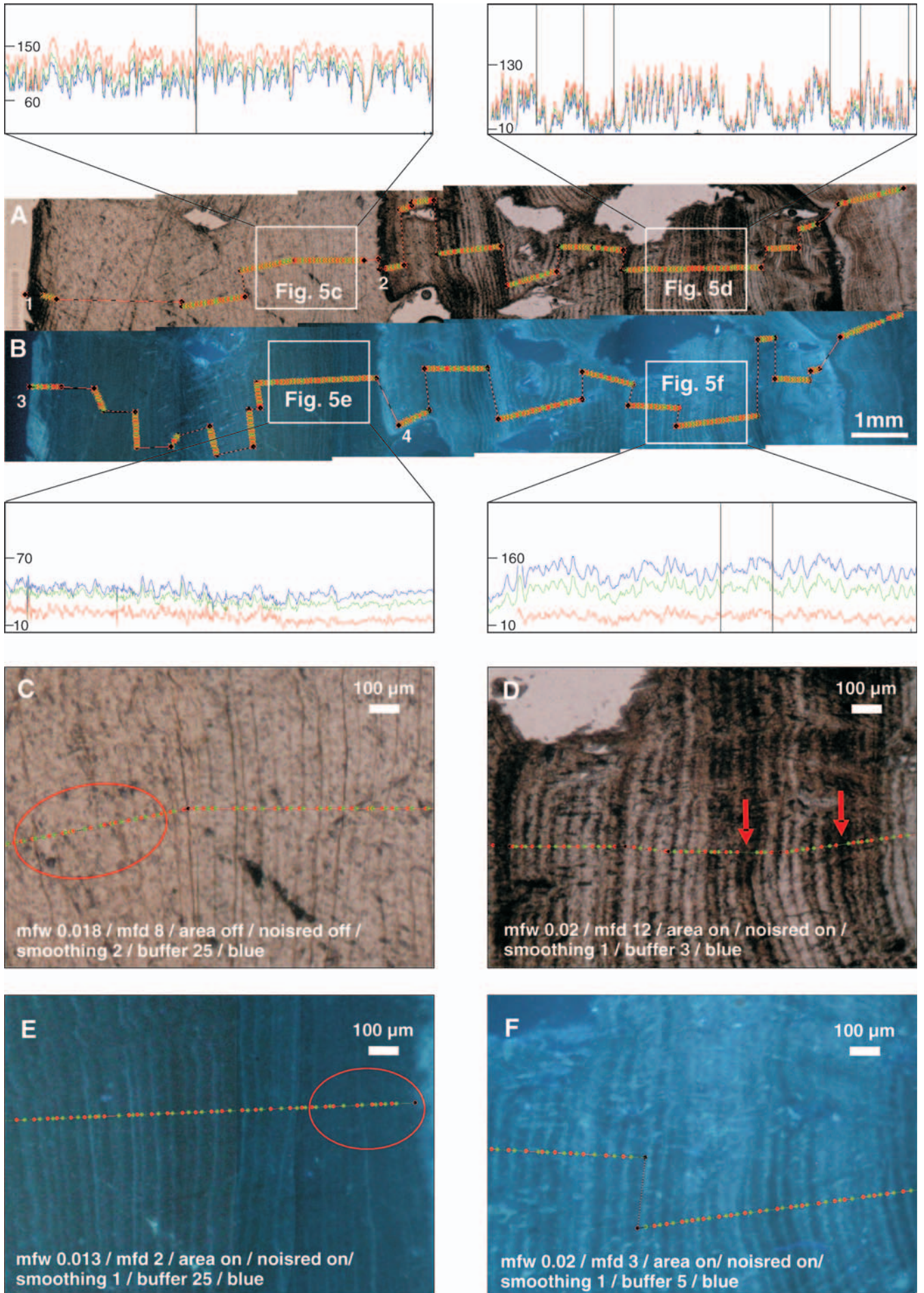
### Lacustrine sediments

The banded lake sediments of the Lisan Formation (Israel, Figure 3C) are composed of aragonite and gypsum layers, alternating with silt and sand detritus (Begin *et al.*, 2004). Lamina thickness in the sample image varies by a factor of 10 from 0.5 mm to 5 mm. The RGB curve oscillates from 160 for the bright aragonite and gypsum to 50 for the dark detrital layers. The highest amplitudes are found in the blue channel. The fb-algorithm yields a total hit rate of 80% and a high accuracy of 98%. The low hit rate is mainly caused by clusters of very closely spaced faintest laminae which are sometimes misinterpreted as individual lamina. In these cases manual readjustment is required.

### Speleothems

Figure 4 shows the annually laminated stalagmite from Savi Cave (Italy; Frisia *et al.*, 2005). Lamina thickness ranges from 10 to 30  $\mu\text{m}$ . Each lamina consists of translucent calcite superimposed by a dark organic-rich calcite layer (S. Frisia, personal communication, 2005). A high frequency signal with amplitude variations of *c.* 100 can be seen in the RGB profile (Figure 4A). The algorithm detects the lamina boundaries with high accuracy (95%) but inclusions are problematic for the fb-algorithm as they are misinterpreted as lamina boundaries (Figure 4B: upper polyline). To overcome this problem we used a high buffer value (buffer size 50 pixel) and selected the course of the polyline to avoid inclusions (Figure 4B: lower polyline). A total hit rate of 90% was achieved. Figure 4D shows the results obtained from the lamination analysis: the absolute number of the real laminae, the thickness of real laminae and the thickness of the semi-laminae versus depth as well as the RGB curve (as mean of the three colour bands).

A long and complex laminated sequence of a Holocene stalagmite (ER 76) from Ernesto cave was analysed to compare our semi-automatically derived results with the manually measured thickness curve of Frisia *et al.* (2003). We obtained two photo-mosaics along a transect line of the thin section. One mosaic was photographed under transmitted light (Figure 5A), the second one under UV-illumination (Figure 5B). In the upper part of the transmitted-light mosaic (the left side of Figure 5A) lamination is composed of thick translucent semi-laminae and the corresponding dark semi-laminae appear extremely faint. The lower part of the transmitted-light image (right side of Figure 5A) is characterized by thick organic-rich dark bands. Using UV-illumination the organic-rich dark semi-laminae fluoresce brightly. In the middle of this sequence a period of condensed deposition occurred around AD 1840, caused by the climate deterioration of the ‘Little Ice Age’ (Frisia *et al.*, 2003). Gaps along the transect line (no data segments) arise from bad lamina preservation and were filled



by data derived from a second photo-mosaic located in an adjacent position on the thin section.

The different types of laminae in the stalagmite are characterized by four sample images as shown by their RGB profiles differing from each other in terms of shape and amplitude (Figure 5A,B). Sharp peaks and high amplitudes prevail in the transmitted-light images and a rather smooth RGB signal with lower amplitudes is observed in the UV images. We used four polylines (1–4 on Figure 5) and tuned the detection parameters of the fb-algorithm for each of these four lamination-types.

The first sample image (Figure 5C) reveals faint and dark semi-laminae that are partly discontinuous and the RGB signal is impaired by a high signal-to-noise ratio. A high buffer value, however, resulted in successful identification of the faint and continuous laminae. In the left part of Figure 5C laminae are highly discontinuous and cannot be successfully identified even using high buffer values. Similarly, manual layer counting also results in large uncertainties in these difficult areas.

In the transmitted-light images the dark organic-rich calcite layers prior to AD 1840 were accurately detected (Figure 5D). Minor readjustments were necessary where these layers are too close together and thus lamina boundaries are missed by the automated detection routine.

Faint and dark semi-laminae are better recognized under UV-illumination (Figure 5E) and all laminae are correctly detected using a high buffer value. However, in the interval of extremely faint and closely spaced laminae (around AD 1840, encircled in Figure 5E), the RGB signal faded (Figure 5B) and the fb-algorithm failed to suggest reasonable lamina boundaries.

The dark organic-rich calcite layers deposited prior to AD 840 fluoresce brightly under UV-illumination and just two lamina boundaries out of 60 are missed by the fb-algorithm (Figure 5F).

Figure 6 compares our semi-automatically derived lamina thickness curve (including manually readjusted lamina boundaries) to the manually measured thickness curve of Frisia *et al.* (2003). The overall fit is satisfactory. Differences between these two curves are attributed to the high growth variability of the stalagmite and the different locations of the transect lines within the thin sections in Frisia *et al.* (2003) and this work. The total hit rates of the transmitted-light profile pre- and post-AD 1840 are 65% (accuracy 80%) and 73% (accuracy 95%), respectively. Where laminae are discontinuous, readjustments were necessary, but the fb-algorithm performed well in the lower laminated part where the thick organic-bearing laminae prevail. The dataset based on the epifluorescence image deviates slightly from the manually measured thickness record of Frisia *et al.* (2003) but follows the instrumental temperature record for which the thickness curve is thought to be a proxy. Accuracies and total hit rates are high for the upper and especially for the lower part of the UV-illuminated photo-mosaic and only minor readjustments were required.

## Discussion

### Tuning the fb-algorithm

The semi-automated approach of the lamination software tool allows the operator to manually adjust lamina boundaries that

have been automatically suggested by the fb-algorithm. Tuning of the fb-algorithm and the course of the user-defined polyline significantly influence the results. Tuning the fb-algorithm is necessary in order to suppress noise, efficiently catch lamina boundaries and to detect closely and widely spaced laminae equally well. The algorithm can be optimized, for example to detect thin laminae by choosing small mfw and mfd values; however, this may produce many surplus boundaries where lamination broadens or the signal-to-noise ratio increases. As a consequence different types of lamination must be treated with different detection and tuning parameters. This requires the polyline to be partitioned into shorter segments, in particular where long and heterogeneously laminated sequences are processed (Figure 5A,B).

### Quality of the RGB or the greyscale signal

As the RGB or greyscale curve constitutes the computational base of the fb-algorithm a minimum quality of the RGB signal is needed to detect lamina boundaries accurately. The minimum quality varies from sample to sample and depends on a variety of parameters, including the shape and size of the RGB features, the signal-to-noise ratio along the polyline, the course of the polyline, the distribution of closely versus widely spaced laminae and optional high buffer values (requires straight laminae). We consider the efficiency of the fb-algorithm is good where both accuracy and total hit rate exceed 70%. In cases where the total hit rate drops below 50% manually digitizing the semi-laminae fully manually is nearly as fast as running the fb-algorithm and subsequently adjusting every second boundary. Where lamination is highly complex, discontinuous, extremely faint or intensively disturbed because of a high signal-to-noise ratio, digitizing the boundaries manually without assistance of the automated fb-algorithm may be a faster approach (eg, Figure 5C,E). A fully manual approach is facilitated by the WinGeol Lamination Tool by digitizing a polyline and placing a node for each lamina boundary. Such a manual segment can be joined with polylines containing data-, no data- and link-segments and the whole laminated sequence can subsequently be exported as one single data file.

A high buffer value is important to accurately detect faint or very thin laminae (Figure 5C,E, Figure 4). The requirements for high buffer values are straight laminae, a low signal-to-noise ratio and a carefully considered course of the polyline (Figure 4B). High buffer values and the *Use Area* parameter significantly improved the result in our test samples.

### Digital images versus counting in the microscope

Counting laminae is usually performed using an optical microscope but this approach becomes impracticable for lamina thickness measurements. We routinely use high quality digital images for lamination analysis as they bear several advantages, especially in cases of microscopic lamination. (1) Digital images allow the operator to laterally compare and cross-correlate laminae easily, which is of importance where lamination is complex, discontinuous or faint. (2) Additional vector and text layers can be introduced, facilitating orientation along long laminated sequences. (3) Multiple and parallel counts along polylines can be performed rapidly on digital images and enhance the robustness of the final results.

The WinGeol Lamination Tool firstly requires acquisition and stitching of the images, which accounts for about

**Figure 5** Performance of the fb-algorithm in a laminated Holocene stalagmite from Ernesto Cave (Italy). (A), (C), (D) Photo-mosaics of sample ER 76 (Frisia *et al.*, 2003) under transmitted light. Top to the left. The period of condensed lamination occurs 6 mm below the top and lasts for about UV illumination. Numbers 1–4 denote four different polylines (see text). (C) Note discontinuous laminae (encircled). (D) Arrows point to missing lamina boundaries. (E) Note condensed and faint laminae inside circle. (F) Profile where the total hit rate and the accuracy are 100%. Sample courtesy S. Frisia and A. Borsato

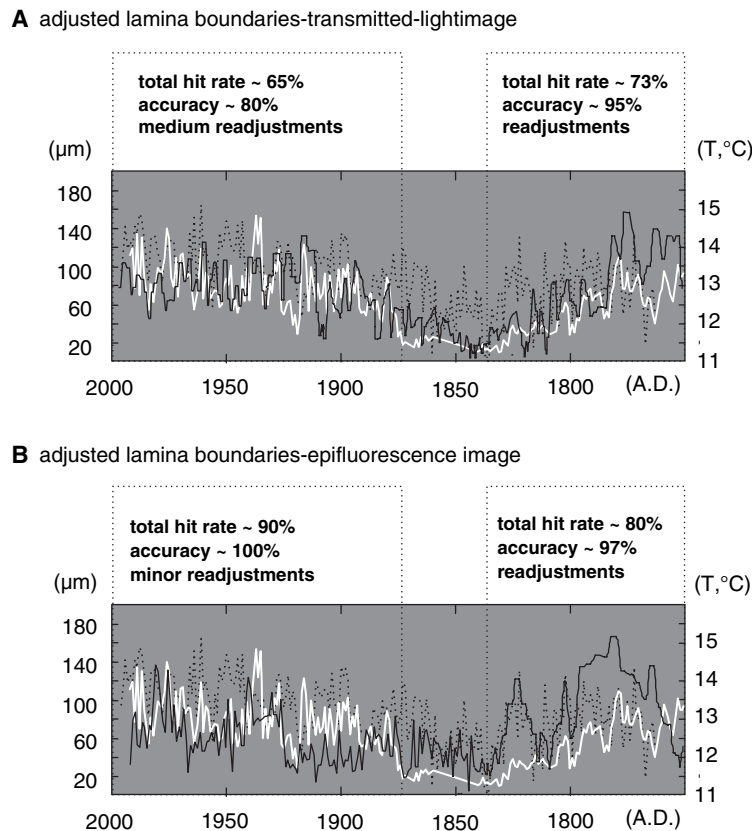


**Figure 6** Manually measured lamina-thickness record of Frisia *et al.* (2003, white curve) compared with semi-automatically derived lamina-thickness curve using the WinGeol Lamination Tool (black curve). Lamina thickness is regarded as a temperature proxy (local temperature record: black dotted line – Frisia *et al.*, 2003)

one-quarter to one-third of the time needed for the entire lamination analysis. Where long laminated sequences require stitching of more than five individual images we use Adobe Photoshop, as this software package provides a very fast algorithm and convenient workflow for that purpose. Acquiring and stitching of digital images can be completely automated using a motorized X-Y microscope stage in conjunction with image processing software that controls the automated scanning process (eg, AnalySIS, Soft Imaging System GmbH; eg, Seelos and Sirocko, 2005).

## Conclusions

Our software is optimized to rapidly process raster data up to one gigabyte in size. Digital images of thin sections or sediment surfaces can be imported and stitched together using the WinGeol lamination tool, thus enabling the operator to efficiently process long laminated sequences.

The WinGeol lamination tool is capable of accurately detecting lamina boundaries within a wide range of laminated archives. Our innovative detection algorithm ‘morphologically screens’ the RGB or greyscale curve for features of a pre-defined size, rather than performing a conventional curve sketch. Best results are obtained by accurately calibrating the detection and tuning parameters for each lamination type. Choosing an appropriate RGB colour channel further improves the results. The limiting factor for the automated detection routine is the quality of the RGB signal (shape, amplitude, signal-to-noise ratio).

Lamination analysis using the WinGeol lamination tool is a semi-automated process and offers a high degree of control to the operator. Profile lines are digitized manually, detected

lamina boundaries can be adjusted individually, and laminae counts and thickness data can be obtained even for archives with high internal growth variability and faint laminae. In addition, thickness variations of semi-laminae are calculated and can be used, eg, as a seasonality proxy. Finally, the software tool enables the operator to rapidly measure multiple and parallel profile lines, enhancing the robustness of the final results.

## Acknowledgements

Software development and MCM were funded by the Austrian Science Fund (Y-122-GEO to CS). We thank M. Kaufmann, N. Waldmann, I. Fairchild, S. Frisia, A. Borsato and B. Schöne for kindly providing sample images and for valuable discussion. A test version of the WinGeol Lamination Tool is available from <http://www.terramath.com> (last accessed 24 May 2006).

## References

- Begin, Z.B., Stein, M., Katz, A., Machlus, M., Rosenfeld, A., Buchbinder, B. and Bartov, Y. 2004: Southward migration of rain tracks during the last glacial, revealed by salinity gradient in Lake Lisan (Dead Sea rift). *Quaternary Science Reviews* 23, 1627–36.
- Conner, S.W., Schowengerdt, R.A., Munro, M. and Hughes, M.K. 2000: Engineering design of an image acquisition and analysis system for dendrochronology. *Optical Engineering* 39, 453–63.
- Fleitmann, D., Burns, S.J., Neff, U., Mudelsee, M., Mangini, A. and Matter, A. 2004: Palaeoclimatic interpretation of high-resolution oxygen isotope profiles derived from annually laminated speleothems from southern Oman. *Quaternary Science Reviews* 23, 935–45.

- Francus, P., Keiming, F. and Besonen, M.** 2002: An algorithm to aid varve counting and measurement from thin-sections. *Journal of Paleolimnology* 28, 283–86.
- Frisia, S., Borsato, A., Preto, N. and McDermott, F.** 2003: Late Holocene annual growth in three Alpine stalagmites records the influence of solar activity and the North Atlantic Oscillation on winter climate. *Earth and Planetary Science Letters* 216, 411–24.
- Frisia, S., Borsato, A., Spötl, C., Villa, I. and Cucchi, F.** 2005: Climate variability in the SE Alps of Italy over the last 17 000 years reconstructed from a stalagmite record. *Boreas* 34, 445–55.
- Hajdas, I., Zolitschka, B., Ivy-Ochs, S.D., Beer, J., Bonani, G., Leroy, S.A.G., Negendank, J.W., Ramrath, M. and Suter, M.** 1995: AMS radiocarbon dating of annually laminated sediments from Lake Holzmaar, Germany. *Quaternary Science Reviews* 14, 137–43.
- Hughen, K.A., Overpeck, J.T. and Anderson, R.F.** 2000: Recent warming in a 500-year palaeotemperature record from varved sediments, Upper Soper Lake, Baffin Island, Canada. *The Holocene* 10, 9–19.
- Hughen, K., Lehman, S., Southon, J., Overpeck, J., Marchal, O., Herring, C. and Turnbull, J.** 2004:  $^{14}\text{C}$  activity and global carbon cycle changes over the past 50 000 years. *Science* 303, 202–207.
- Ojala, A.E.K. and Alenius, T.** 2005: 10 000 years of interannual sedimentation recorded in the Lake Nautajärvi (Finland) clastic-organic varves. *Palaogeography, Palaeoclimatology, Palaeoecology* 219, 285–302.
- RinnTech** 2002: *LignoVision<sup>TM</sup> Scientific software for automated tree-ring measurements and density profiling v.1.32—software manual*. <http://www.rinntech.de> (last accessed 28 April 2006).
- Schaaf, M. and Thurow, J.** 1994: A fast and easy method to derive highest-resolution time-series datasets from drill cores and rock samples. *Sedimentary Geology* 94, 1–10.
- Seelos, C. and Sirocko, F.** 2005: RADIUS – rapid particle analysis of digital images by ultra-high-resolution scanning of thin sections. *Sedimentology* 52, 669–81.
- Varem-Sanders, T.M.L. and Campbell I.D.** 1996: *Dendroscan a tree-ring width and density measurement system*. Special Report 10, UBC Press.
- Zolitschka, B.** 1996: High resolution lacustrine sediments and their potential for paleoclimatic reconstruction. In Jones, D.P., Bradley, R.S. and Jouzer, J., editors, *NATO ASI series – climatic variations and forcing mechanisms of the last 2000 years*. Springer, 444–78.
- 1998: A 14 000 year sediment yield record from western Germany based on annually laminated lake sediments. *Geomorphology* 22, 1–17.

Copyright of Holocene is the property of Arnold Publishers and its content may not be copied or emailed to multiple sites or posted to a listserv without the copyright holder's express written permission. However, users may print, download, or email articles for individual use.